Detection and Estimation of Local Signals

Xiao Fang
Department of Statistics, The Chinese University of Hong Kong and
David Siegmund
Department of Statistics, Stanford University
April 15, 2020

Abstract

We study the maximum score statistic to detect and estimate local signals in the form of change-points in the level, slope, or other property of a sequence of observations, and to segment the sequence when there appear to be multiple changes. We find that when observations are serially dependent, the change-points can lead to upwardly biased estimates of autocorrelations, resulting in a sometimes serious loss of power. Examples involving temperature variations, the level of atmospheric greenhouse gases, suicide rates and daily incidence of COVID-19 illustrate the general theory.

Keywords: segmentation, change-point, broken line, autoregression.

1 Introduction.

We consider a problem of detection, estimation, and segmentation of local nonlinear signals imbedded in a sequence of observations. As a model, we assume for u = 1, ..., T

$$Y_u = \rho Y_{u-1} + \mu(X_u) + \sum_k \xi_k f[(X_u - t_k)/T] + \epsilon_u,$$
(1)

where $t_1 < t_2 < \ldots < t_M$ define the locations and f the "shape," of the local signals. For asymptotic analysis given below, we assume that the t_k are scaled, so $t_k/T = t_{0,k}$. Initially we assume the X_u are fixed, but for some applications they are random. The ϵ_u are independent mean 0, normally distributed errors. For the moment we assume their variances are known and equal one, and discuss later how they should be estimated. The nuisance parameters $\mu(X_u)$ depend on the variable X_u and may be constant or a parameterized regression function. They might, for example, be the mean values for a control group, for which it is assumed that all of the $\xi_j = 0$. For our general theory we assume ρ is an unknown constant, but we estimate ρ differently in different problems.

An important special case that we return to in examples below is $X_u = u$ and $\mu_u = \alpha + \beta[(u - (T+1)/2)/T]$, so with this notation the model becomes

$$Y_u = \rho Y_{u-1} + \mu_u + \sum_k \xi_k f[(u - t_k)/T] + \epsilon_u.$$
 (2)

It is occasionally convenient to simplify several basic calculations by considering an alternative continuous time model, for which (2) can be conveniently written

$$dY_u = -\gamma Y_u du + \mu_u du + \sum_k \xi_k f[(u - t_k)/T] du + dW(u)$$
(3)

for $0 \le u \le T$, where dW defines white noise residuals.

Specific choices of the function f appear to be appropriate for a number of applications, some of which are discussed below. The special case $f(x) = I\{x > 0\}$ is a frequently discussed "change-point" model, which has been applied to a variety of problems, usually with ρ assumed equal to 0. See, for example, Olshen et al. (2004), Robbins, Gallagher, and Lund (2016) and references given there. Fang, Li and Siegmund (2018) and Fryzlewicz (2014) address a version of the problem that involves the possibility of multiple change-points, and a major goal is segmentation of the observations to identify their number and locations, while controlling the probability of false positive detections. In this paper we extend the methods of Fang, Li and Siegmund (2018) to deal with more general signals and with observations that may have autoregressive dependence. See also Baranowski, Chen, and Fryzlewicz (2019).

An interesting special case is a broken line regression model, where $f(x) = x^+$, so the model is given by

$$Y_u = \rho Y_{u-1} + \alpha + \beta [(u - (T+1)/2)/T] + \sum_{k} \xi_k [(u - t_k)^+/T] + \epsilon_u.$$
 (4)

This model has a long history, again primarily for the case of independent observations and at most one break-point in a regression line. An application to monitor kidney function after transplant has been discussed in a series of papers by A. F. M. Smith and others (e.g. Smith and Cook (1980)). Davies (1987) and Knowles and Siegmund (1989) give theoretical analyses for independent observations. Toms and Lesperance (2003) provides an analysis and ecological applications. Several of the examples discussed below involve climatological time series, or day by day newly confirmed cases of COVID-19. Although alternative models are possible, a broken line model provides a conceptual framework that allows us to fit an easy to understand model and to ask whether the breakpoints represent changes of scientific importance.

In a variety of genomic applications t denotes a genomic location, and different applications suggest functions f having different characteristic shapes. For example, for detection of copy number variations (CNV) the indicator of an interval or a half line may be appropriate. For detection of differentially methylated genomic regions Jaffe, et al. (2012a) suggests a "bump" function. See simple examples below and elaborations of this model involving covariates in Jaffe, et al. (2012b). For ChIP-Seq analysis steeply decaying symmetric functions like $(1 - |u|)^+$, $\exp(-|u|)$, or a normal probability density function are different possibilities (cf. Shin et al. (2013), Schwartzman et al. (2013)). In some applications it is often appropriate to add a scale parameter τ , so at u the signal located at t is of the form $\xi f[(u-t)/(\tau T)]$ (cf. Siegmund and Worsley (1995)). The model of "paired change-points" of Olshen et al. (2004) can be described similarly, with $f(x) = I\{0 < x \le 1\}$.

In the special case that μ is a constant, $X_u = Y_{u-1}$, and f(x) is the indicator that $x \leq 0$, (1) is the simplest example of a threshold autoregression, as introduced by Tong and studied by Chan and Tong and others (e.g., Chan and Tong (1990)) in numerous projects. In a still different context, X_u may be a regressor, say a biomarker, and the local signal can be used to study whether a subset of individuals, defined by the value of that biomarker, differ from others in some respect, e.g., response to a treatment.

In some applications X_u may be multidimensional or the noise distribution may not be normal, with the Poisson distribution representing a particularly interesting alternative.

Although the focus or our paper is on segmentation of multiple signals, we also develop confidence regions for t and jointly for t and ξ . After beginning with some basic calculations and a discussion of testing for at most one change in Section 2, segmentation is discussed in Section 3 and illustrated in 3.1. New approximations to control the false positive error rate given in Section 3, which combine smooth and not smooth stochastic processes, play

an important role. Sections 4 and 5 briefly consider a number of other special cases of our general framework. Additional theory and examples are contained in an online Supplement.

We have used simple models to minimize issues of over-fitting and data re-use that could arguably complicate interpretation of our segmentations. Once segmented, the models become simple linear models, so we also consider a second stage analysis to estimate more accurately the nuisance parameters and the ξ_j , which then allows us to re-evaluate the accuracy of the segmentation.

Although large sample theory suggests use of maximum likelihood estimators to estimate the nuisance parameters ρ and σ^2 , we find that in some cases the signals themselves introduce large bias into those estimators. We discuss some ad hoc alternatives below.

2 Basic Calculations and the Case of at Most One Change.

To introduce our notation and provide some basic results, we begin with the model given by (2), with M=1 or 0, and we consider a test of the hypothesis $\xi=0$. The log likelihood is given by $\ell(\xi,t,\theta)$

$$= -.5 \sum_{u} \{Y_u - \rho Y_{u-1} - \alpha - \beta [(u - (T+1)/2)/T] - \xi f[(u-t)/T] \}^2,$$

where $\theta = (\alpha, \beta, \rho)'$, and we consider a test based on the maximum with respect to t of the standardized score statistic

$$\ell_{\mathcal{E}}(0, t, \hat{\theta}) / \sigma(t),$$
 (5)

where $\ell_{\xi} = d\ell/d\xi$ and $\hat{\theta}$ is the maximum likelihood estimator of the nuisance parameters under the hypothesis $\xi = 0$; and $\sigma^2(t)$ is the asymptotic variance of the numerator.

We begin with the standard large sample expansion of the numerator in (5) given by

$$\ell_{\xi}(0, t, \hat{\theta}) \approx \ell_{\xi}(0, t, \theta) - I_{\xi, \theta} I_{\theta, \theta}^{-1} \ell_{\theta}, \tag{6}$$

where $I_{\cdot,\cdot}$ denotes elements of the Fisher information matrix and by the law of large numbers all quantities on the right hand side are evaluated at $\xi=0$ and true values of the other parameters. This expansion is valid in large samples up to terms that are o(T) in probability. To emphasize the structure of this approximation we find it convenient to use the notation \mathbb{E}_0 to denote expectation under the hypothesis $\xi=0$ and write (6) in the form $V_t=\ell_{\xi}(t)-\Psi(t)'A\ell_{\theta}$, where $\ell_{\xi}(t)=\ell_{\xi}(0,t,\theta)$, $\Psi(t)'=\mathbb{E}_0[\ell_{\xi}(t)\ell'_{\theta}]$ is not random although it depends on t; ℓ_{θ} does not depend on t, and under the hypothesis $\xi=0$ it has mean value 0 and covariance matrix $A^{-1}=I_{\theta,\theta}$.

Remark. It may be shown that the decomposition given in (6) does not depend on the normality of the ϵ_j , although we can no longer use the terminology of likelihood, efficient score, etc., and must rely on the central limit theorem to justify the asymptotic normality of probability calculations given below. The special case of Poisson observations is discussed briefly in Section 5.

Calculations yield a number of simple propositions.

Proposition 1.

$$\Sigma(s,t) = \mathbb{E}_0(V_s V_t) = \mathbb{E}_0[\ell_{\xi}(s)\ell_{\xi}(t)] - \Psi(s)' A \Psi(t). \tag{7}$$

In particular the variance of V_t is $\sigma^2(t) = \Sigma(t, t)$.

Remark. In the case the local signal contains a scale parameter, so it takes the form $\xi f[(u-t)/(\tau T)]$, the covariance is similar in its general formulation, but slightly more complicated to compute in examples.

Writing $\mathbb{E}_{t,\xi}$ to denote expectation under the alternative, where t and ξ can be vectors, we have

Proposition 2. $\mathbb{E}_{t,\xi}(V_s) = \sum_k \Sigma(s,t_k) \xi_k$.

Let $Z_t = [\ell_{\xi}(t) - \Psi(t)'A\ell_{\theta}]/\sigma(t)$, and consider the test statistic $\max_t |Z_t|$. The false positive probability for the test that detects a signal when $\max_t |Z_t|$ is large is given by $\mathbb{P}_0\{\max_t |Z_t| \geq b\}$.

To evaluate this probability, we distinguish essentially two cases, one where f is continuous and the second where it is discontinuous. The case where f is the indicator of a half line or an interval (of unspecified length) is discussed in Fang, Li and Siegmund (2018). Here we assume that f is continuous and piecewise differentiable. An approximation based on Rice's formula is given by

Proposition 3.

$$\mathbb{P}_0\{\max_{T_0 \le t \le T_1} |Z_t| > b\} \le 2\{(\varphi(b)/(2\pi)^{1/2}) \int_{T_0}^{T_1} [\mathbb{E}_0(\dot{Z}_t)^2]^{1/2} dt + 1 - \Phi(b)\},\tag{8}$$

where \dot{Z}_t denotes the derivative of Z at t. For the model where the local signal at u has the form $\xi f[(u-t)/\tau T]$, and we maximize over both t and a range of values of τ , a first order approximation becomes

$$\mathbb{P}_0\{\max_{t,\tau}|Z_{t,\tau}| > b\} \approx 2\{b\varphi(b)/(2\pi)\} \int_{\tau_0}^{\tau_1} \int_{T_0}^{T_1} \det[\mathbb{E}_0(\dot{Z}\dot{Z}')]^{1/2} dt d\tau, \tag{9}$$

where $\dot{Z} = \nabla Z_{t,\tau}$. This approximation can be improved by adding terms involving edge effects and corrections for curvature. The most important is the boundary correction at the minimum value of τ , which equals $(8\pi)^{-1/2}\varphi(b)\int_{T_0}^{T_1} [\mathbb{E}_0(\dot{Z})^2]^{1/2} dt$, where now $\dot{Z} = \frac{\partial Z}{\partial t}(t, \tau_0)$. It is often convenient when T is large to ignore edge effects, which simplifies integration over

 $[T_0, T_1]$. See Siegmund and Worsley (1995) or Adler and Taylor (2007) for more detailed approximations.

To evaluate (8) and (9), the following result is useful.

Proposition 4.

$$\mathbb{E}_0[(\dot{Z}\dot{Z}')] = [\mathbb{E}_0(\dot{\ell}\dot{\ell}') - \dot{\Psi}'A\dot{\Psi}]/\sigma^2(t) - [\dot{\sigma}\dot{\sigma}']/\sigma^2. \tag{10}$$

Finally observe that by Propositions 1 and 2, we have the "matched filter" conditions, and consequently

Proposition 5. Given t (or t, τ), the variable V_t (or $V_{t,\tau}$) is sufficient for ξ .

For the specific case of (4), it simplifies calculations somewhat to consider the continuous time version given in (3), which amounts to replacing certain sums by integrals, leading to

Proposition 6.
$$\sigma^2(t) \sim T\{(1-t_0)^3/3 - (1-t_0)^4(1+t_0+t_0^2)/3\}$$
, and $\mathbb{E}_0(\dot{V}_t^2) \sim T\{(1-t_0) - (1-t_0)^2 - 3[t_0(1-t_0)]^2\}$.

As expected, this result does not depend on the nuisance parameters α , β . It is perhaps surprising that it also does not depend on ρ . See the online Supplement for details.

2.1 Confidence Regions

It is possible to obtain a confidence region for the parameters t or a joint region for t and ξ . Calculation shows that the expected value of V_s equals ξ times the covariance of V_s and V_t (cf. Proposition 2). An easy consequence is that $Z_t = V_t/\sigma(t)$ is sufficient for ξ , so the conditional distribution of Z_s given Z_t is the same as it would be under the null hypothesis, $\xi = 0$.

Now we must consider two cases, depending on whether the process has a jump at t. The case of a jump was studied by Fang, Li and Siegmund (2018), so here we consider

the continuous case. For a similar approach based on a different probability evaluation see Knowles, Siegmund and Zhang (1991). We use the Kac-Slepian model process, which for a mean 0 unit variance stationary, differentiable, Gaussian process, say U_s , gives a parabolic approximation for the process in a neighborhood of s_0 conditional on U_{s_0} assuming a large value. As a consequence of those arguments, in a neighborhood of s_0

$$U_s = U_{s_0} + (s - s_0)\dot{U}_{s_0} - \frac{(s - s_0)^2}{2}U_{s_0}\mathbb{E}_0[(\dot{U}_{s_0})^2] + o((s - s_0)^2),$$

SO

$$\max_{s}(U_s^2 - U_{s_0}^2) \approx \dot{U}_{s_0}^2 / \{\mathbb{E}_0[(\dot{U}_{s_0})^2]U_{s_0}\},\tag{11}$$

with errors that converge to 0 in probability. It follows that the conditional distribution of $\max_s(Z_s^2 - Z_t^2)$ is asymptotically χ^2 with one degree of freedom, so a $1 - \alpha$ confidence region is given by the set of all s that satisfy $Z_s^2 \geq Z_t^2 - \chi_{1-\alpha}^2$, where $\chi_{1-\alpha}^2$ is the $1 - \alpha$ quantile of the χ^2 distribution with one degree of freedom. This is in effect the same result one would obtain by inverting the log likelihood ratio statistic if Z were the log likelihood of a parameter satisfying standard regularity conditions.

A joint confidence region for ξ and t is also easily obtained. To the condition that Z_t^2 must be within a given distance of $\max_s Z_s^2$, we also require that $|Z_t - \xi \sigma(t)|$ is sufficiently small. The pairs ξ , t that satisfy $\max_{\delta} [Z_{t+\delta}^2 - Z_t^2] + (Z_t - \xi \sigma(t))^2 \le c^2$ provide a joint confidence region having the confidence coefficient

$$\mathbb{P}_{t,\xi} \{ \max_{\delta} [Z_{t+\delta}^2 - Z_t^2] + (Z_t - \xi \sigma(t))^2 \le c^2 \}$$
 (12)

$$= \mathbb{E}_{t,\xi} \left[\mathbb{P}_{t,\xi} \left\{ \max_{\delta} [Z_{t+\delta}^2 - Z_t^2] \le c^2 - (Z_t - \xi \sigma(t))^2 | Z_t \right\}; |Z_t - \xi \sigma(t)| \le c \right]$$
 (13)

which equals the distribution of a χ^2 random variable with two degrees of freedom, again as if standard regularity conditions had been satisfied.

Looking ahead to the possibility of finding joint confidence regions for two (or more) change-points $t_1 < t_2$, we face a more subtle argument. First note that with $t = (t_1, t_2)$, and $\xi = (\xi_1, \xi_2)$, a straightforward calculation extending the result given in Proposition 2 (cf. (29) in the online Supplement) shows that $\mathbb{E}_{t,\xi}(V_s) = \sum_i [\xi_i \sigma(t_i) \Sigma(s, t_i)]$, where $\Sigma(s, v) = \mathbb{C}ov(V_s, V_v)$. This produces by a second calculation the conclusion that the log likelihood of V_s , $s = 1, \dots, T$ equals $\sum_i \xi_i \sigma(t_i) V_{t_i} - .5 \sum_{i,j} \xi_i \xi_j \sigma(t_i) \sigma(t_j) \Sigma(t_i, t_j)$. Hence the log likelihood ratio statistic, given t, for testing that ξ is the 0 vector equals

$$(V_{t_1}, V_{t_2}) \Sigma(t_1, t_2)^{-1} (V_{t_1}, V_{t_2})' = ||\tilde{Z}_{t_1, t_2}||^2,$$
(14)

where $\tilde{Z}_{t_1,t_2} = \Sigma(t_1,t_2)^{-1/2}(V_{t_1},V_{t_2})'$ has a standard bivariate normal distribution when $\xi = 0$, and $||\cdot||$ denotes the Euclidean norm. It follows from sufficiency and the Kac-Slepian argument used above that

$$\max_{\delta_1, \delta_2} [||\tilde{Z}_{t_1+\delta_1, t_2+\delta_2}||^2 - ||\tilde{Z}_{t_1, t_2}||^2]$$

has a χ^2 distribution with two degrees of freedom and can be used as above to obtain a joint confidence region for (t_1, t_2) .

A joint confidence region for t, ξ follows by an argment similar to that given above.

Remark. The confidence regions for the change-points are easy to visualize and seem reasonable. The estimates of ξ are more problematic, since selection of the change-point value t introduces bias into the estimation of ξ which may be exacerbated by a biased estimate of ρ . In Section 3 we consider a different method for estimating the parameters ξ .

2.2 Numerical Examples

We begin with several simple numerical examples of broken line regression, which differs from some other models in the sense that a change of slope can have a lasting effect that makes even a relatively small change easy to detect if it persists.

Example 1. Extreme Precipitation in the United States. Extreme precipitation in the United States is reported by the National Oceanographic and Atmospheric Administration (NOAA) at

https://www.ncdc.noaa.gov/temp-and-precip/uspa/wet-dry/0.

This web site gives the area of the country where monthly rainfall exceeded the 90th percentile of normal for the 124 years and 8 months beginning in 1895.

Our test for at most one changes suggests a slope increase in 1954, with a p-value of 0.001. The value of ρ is estimated to be 0.08. The test applied to extremely low precipitation (area of the country below the 10th percentile) is consistent with the hypothesis of no change in slope.

Example 2. Central England Annual Average Temperature. The average temperature in central England England from 1659 (Manley (1974)) until 2019 is reported on

(https://www.metoffice.gov.uk/hadobs/hadcet/cetml1659on.dat).

The maximum Z value is about 4.60, with ρ estimated to be 0.16, and occurs in 1969. The appropriate (two-sided) p-value is about 6×10^{-5} . See Figure 1, where it appears that there might also be earlier change-points. Although the mercury thermometer was relatively young in 1659, those early years are interesting since they appear to involve the "little ice age." We return to these data below for our discussion of segmentation. Meanwhile it may be interesting to note that an approximate 95% confidence region based on the detected change in 1969 is (1895,1990), which reflects the local shape of the plot in Figure 1 and suggests the possibility that an increase in temperature may have actually begun during the late 19th century.

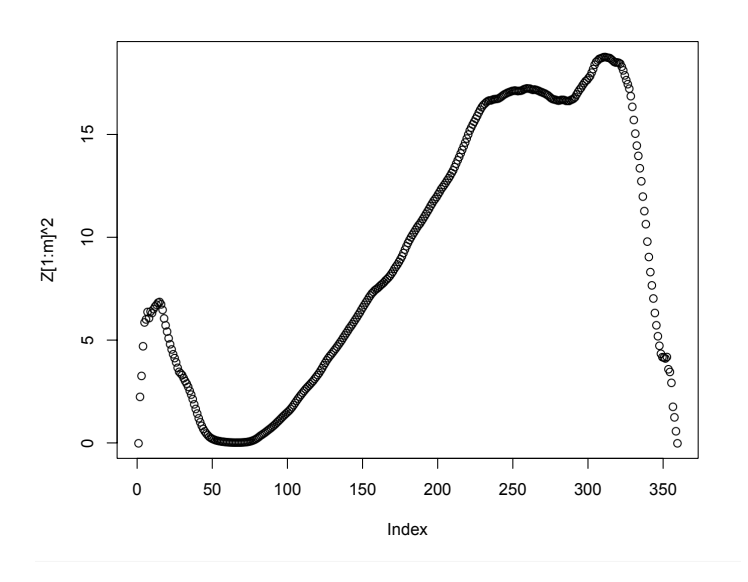


Figure 1: Plot of \mathbb{Z}_t^2 for central england temperature data, 1659-2017.

2.3 Estimation of σ^2 and ρ : A Simulated Example.

Although we have assumed the variance known in our theoretical calculations, in our numerical studies we have estimated it by the residual mean square under the null hypothesis. Other possibilities when the data are independent are sums of squares of first or second order differences: $\sum_{u} (Y_{u+1} - Y_u)^2 / 2m$ or $\sum_{u} (Y_{u+1} - 2Y_u + Y_{u-1})^2 / 6m$, which may be preferable. First order differences remove most of the effect of changing mean values, and second order differences also mitigate the effect of slope changes.

Regarding correlation of the observations, a useful model is one that helps to control false positive errors with minimal loss of power; and to that end our working model is a first order autoregression. Using a value of ρ that is too small can lead to an increase in false positives. But when there are change-points, the maximum likelihood estimator of ρ under the null hypothesis that $\xi = 0$ can be upwardly biased, leading to a loss of power, as we can easily see from the simulated data described below.

The simulated example in Table 1 illustrates the problem of estimating ρ and the effect on the power to detect a change.

For the data in the third and fourth rows of the Table, if we assume it known that $\rho = 0$ and use second order differences to estimate σ^2 , the estimated value is 0.89 and the maximum Z value is 6.77. In all cases, the maximizing value of t is 94. In most other cases as well the maximizing value of t provides a reasonable estimator of the true value.

It is clear from these examples and others not shown that the existence of a change-point causes the estimator of ρ to be upwardly biased and results in a loss of power compared to using the true value of ρ . This is usually worse if there are multiple change-points. If a plot of the data indicates long stretches without change-points, one might use an estimator of ρ from that segment. For the data in the next to last row of Table 1, an estimate of ρ based on

Table 1: Simulated examples: m=150,, 0.05 threshold is b=2.83. Locations of breakpoints and changes in the slope occurring at the break-points are as indicated. Rows where $\hat{\rho}$ has been set equal to ρ are included to illustrate the loss of signal that occurs because of bias in estimation of ρ .

t	ξ	ρ	$\hat{ ho}$	$\hat{\sigma}$	$\max_s Z_s$
	0.00	0.50	0.48	0.98	1.60
	0.00	0.60	0.56	0.98	1.05
100	0.05	0.0	0.30	1.04	4.04
100	0.05	0.0	0.00	1.09	5.51
100	0.05	0.4	0.60	1.19	3.86
100	0.05	0.6	0.75	1.00	3.34
100	0.05	0.6	0.60	1.02	5.06
50	0.04	0.5	0.54	0.97	3.37
50	0.04	0.5	0.50	0.97	3.66
50	-0.033	0.6	0.76	1.15	2.74
50	-0.033	0.6	0.60	1.15	4.34

the observations 65-150 yields the value 0.61, which in turn leads to a maximum Z-value of 4.31. Although the theory developed here does not justify this approach, numerous simulations suggest that it works reasonably well.

A second consideration in estimation of ρ is robustness of our procedure against more complex forms of dependence. Without exploring this question in detail, consider again the next to last row of Table 1, but where there is a second order autoregressive coefficient of - 0.2 and $\xi = -0.06$. A simulation of this case gives an estimator of ρ equal to 0.6 based on all the data, with a maximuom Z-value of 3.32, and an estimator equal to 0.42 based on the second half of the data, with a maximum Z-value of 4.85. Other simulations, not given here, suggest that at least for higher order autoregressive dependence, the first order model we have suggested provides reasonable protection against an inflated false positive error rate.

A different approach (e.g., Robbins, Gallagher, and Lund (2016)) for dealing with dependence in the standard change-point model (i.e., $f(s) = I\{s > 0\}$) is to assume that the estimated residuals from a least squares fit of the null model form a locally dependent stationary process and estimate the autocovariances accordingly. Weak convergence arguments typically indicate that a rescaled process converges weakly to a Gaussian process, often related to a Brownian Bridge, which can be studied to look for change-points. Although this method has some advantages, we prefer our approach for facilitating quantitative statements in the form of hypothesis tests and confidence intervals after a minimal amount of "data snooping" to arrive at a useful model. If we are successful in detecting the signal locations, our model for the other parameters becomes a standard linear model. In Section 3.1 we discuss analysis of this linear model as a test of our approach.

3 Segmentation.

We now turn to the problem of segmentation when there may be several change-points. It is helpful conceptually to think of two different cases. In the first the signals exhibit no particular pattern. In the second two or more changes are expected to produce a definite signature. For the problem of changes in levels of the process, paired changes frequently take the form of an abrupt departure from followed by a return to a baseline level.

Here we initially concentrate on the case of signals having no apparent pattern and consider versions of the two methods suggested in Fang, Li and Siegmund (2018) for detection of jump changes. First we consider a pseudo-sequential procedure, called Seq below, where it is convenient to write Z(t,T) to denote the statistic Z(t) when the interval of observation is [0,T]. We also use a minimum sample size m_0 and a minimum lag n_0 , both of which we often set equal to 5. Let $t_0 = m_0$ and let T be the smallest integer exceeding $t_0 + n_0$ such that for some $t_0 < t < T - n_0$, the value of Z(t,T) exceeds a threshold b to be determined by a constraint on the probability of false positive error. The first change-point is taken to be t_1 : equal to $\arg \max |Z_t|$, or the smallest or largest value of t for that smallest T. (In numerical experiments we have been unable to find a consistent preference.) The process is then iterated starting from t_1 . The nuisance parameter ρ is assumed to be known. In practice it is estimated from the data or more often from a subset of the data to mitigate the effect of the bias discussed above. The other nuisance parameters, are estimated from the current, evolving interval of observations, so that the nuisance parameters associated with one change-point do not confound detection of another. It would also be possible to estimate ρ from the currently studied subset of the data, but this estimator appears to be unstable.

To control the global false positive error rate, we want an approximation for

$$Q = \mathbb{P}\{ \max_{m_0 < t < T - n_0, T \le m} |Z(t, T)| \ge b \},\$$

where m is the number of observations and m_0, n_0 represent minimal sample sizes, both of which we frequently take to be 5. To emphasize that T is a variable quantity, we also write $\sigma^2(t,T), \Psi(t,T)$, etc.

Let
$$\beta(t,T) = \{\mathbb{E}[V\partial V/\partial T) - .5\partial \sigma^2(t,T)/\partial T\}/\sigma^2(t,T) \text{ and } \lambda_t = \mathbb{E}[(\dot{Z}_{t,T})^2].$$
 Then

$$Q \approx (2/\pi)^{1/2} b\varphi(b) \sum_{T=m_0}^{m} \int_{m_0 < t \le T - n_0} \{ \lambda_t \beta(t, T) \nu [b(2\beta(t, T))^{1/2}] \}^{1/2} dt.$$
 (15)

A derivation of the approximation (15) begins from the initial approximation of the probability of interest by a sum over T of the sum over $t \leq T - n_0$ of the integral over x from 0 to ∞ of the product of three factors: (i) $\mathbb{P}\{Z(t,T) \in b + dx/b\} \approx \varphi(b) \exp(-x) dx/b$; (ii) $\mathbb{P}\{Z(t-\delta,T) < b|Z(t,T) = b + x/b\}$; and (iii) $\mathbb{P}\{\max_{j\geq 1} b[Z(t,T-j) - Z(t,T)] < -x|Z(t,T) = b + x/b\}$.

The second factor is approximately $\Phi[\delta b \lambda_t^{1/2} - x/(\delta b \lambda_t^{1/2})]$. If we choose δ , so that δb is very small, the integral is dominated by small values of x. The third factor is approximately $\mathbb{P}\{\max_j S_j \leq -x\}$, for a suitable random walk. For small x, it is approximately $\mathbb{P}\{\max_j S_j < 0\}$. Putting these two observations together leads to the approximation given by (15).

A slightly more complex calculation leads to a different and apparently preferable approximation, which is based on a similar analysis but incorporates in addition the conditional probability, given Z(t,T) = b + x/b, that $2b[\max_s Z(s,T) - Z(t,T)] \in dy$ and $b[Z(t,T-j) - \max_s Z(s,T)] < -(x+y)$ for all $j \geq 1$. By virtue of the Kac-Slepian model process $2b[\max_s Z(s,T) - Z(t,T)] \sim \dot{Z}(t,T)^2/\mathbb{E}\dot{Z}(t,T)^2$ and hence is an independent χ_1^2

random variable. This leads to an expression similar to (15), but with the integrand in (15) replaced by

$$b\lambda_t^{1/2}\beta(t,T)\nu\{b[2\beta(t,T)]^{1/2}\}.$$
(16)

In spite of its somewhat different appearance, this second approximation is slightly less conservative than the first, but gives very similar numerical values. For $m_0 = n_0 = 3$ and m = 250, the first approximation gives a 0.05 threshold of 4.08, while the second gives 3.97. Since these probabilities vary substantially for small values of m_0 , n_0 , and neighboring changes in slope seem difficult to detect and rarely to occur in the data we have studied, we typically use the values $m_0 = n_0 = 5$, which for this example would reduce the 0.05 threshold given by (16) from 3.97 to 3.89.

The approximation (16) may be used to assign a p-value to the the individual detections. For example, suppose we use the threshold b = 4.09, which for $m_0 = n_0 = 5$ and m = 500 gives a global false positive error of 0.05. Suppose also that we detect a change at t = 50 with T = 70 and Z(50, 70) = 4.49. The approximation (16) for m = 70 and b = 4.49, which equals 0.001, can be regarded as a p-value for that detection. This argument can be applied iteratively to obtain p-values for a second and subsequent detections. In view of the lag between a putative change-point t and the value of t when detection occurs, it is possible for the sum of p-values to exceed the global significance value, although numerical experimentation indicates that this rarely occurs.

When this process detects a change in slope, for the smallest value of T there typically is a cluster of values of t where |Z(t,T)| exceeds the chosen threshold. In practice we might reasonably choose the smallest such t, or the value that maximizes |Z(t,T)|. We then iterate the process starting from the selected t. Upon iteration the background linear regression is estimated using the data beginning with that t. It may not be clear which

choice is better in a particular application.

Remarks. (i) Although we use this "pseudo-sequential" method with a given amount of data, it can also be used for actual sequential detection, as in the problem of monitoring kidney transplants discussed in Smith and Cook (1980).

(ii) Although sample paths of the process Z(t,T) as a function of t are smooth, as a function of T they behave locally like a random walk. A consequence is that to obtain a mathematically precise derivation of the approximation (15), local perturbations of the paramter T must be scaled by a small factor, say Δ , which converges to 0 at the rate of $1/b^2$ when $b \to \infty$. See, for example, Fang, Li and Siegmund (2018) for the case of abrupt changes in the mean. A similar remark applies to (17) given below.

A second method of segmentation, called MS below (for Maximum Score Statistic), uses (in obvious notation)

$$\max_{m_0 < T_0 < t < T_1 < m} Z_{T_0, t, T_1}.$$

An asymptotic approximation to the null probability that this expression exceeds b can be computed by a modification of the argument behind (16), and we obtain the approximating expression

$$\left(\frac{2}{\pi}\right)^{1/2}b^2\varphi(b)\times$$

$$\sum_{m_0 \le T_0 < T_1 \le m} \int_{T_0 < t < T_1} (\lambda_t)^{1/2} \beta_0(t, T_0) \beta(t, T_1) \nu\{b[2\beta_0(t, T_0)]^{1/2}\} \nu\{b[2\beta(t, T_1)]^{1/2}\} dt, \quad (17)$$

where $\beta_0(t, T_0)$ is defined similarly to $\beta(t, T)$. The evaluation of (17) can be simplified by a summation by parts and the observation that the various functions of three variables, (T_0, t, T_1) , occurring in (17) are in fact functions of two variables: $(t - T_0, T_1 - T_0)$.

These methods determine a list of putative local signals together with generally overlapping backgrounds. We consider different algorithms for selecting a set of local signals and backgrounds from this list, with a preference for the additional constraint that no background overlap two local signals. In Fang, Li and Siegmund (2018) examples of particular interest were the shortest background, (cf. also Baranowski, Chen, and Fryzlewicz (2019)), and the largest Z value. For the second of these methods we have paid in advance for false positive errors, so we can also consider other methods for searching the list, e.g., subjective consistency with a plot of the data. We also find it convenient computationally to follow the suggestion of Fryzlewicz (2014) by searching a random subset of intervals, which seems to work very well. When it appears that the number of changes is small, as in the examples considered in this paper, one might also use a combination of methods, e.g., searching a small random subset of intervals at a low threshold to generate candidates, then sorting those by hand with tests to detect at least one change at the appropriate higher threshold.

The methods discussed so far are "bottom up" methods in the sense that they attempt to identify one local signal at a time against a background appropriate for that signal. A popular "top down" method in the change-point literature scans all the data looking for a pair of change-points (e.g., Olshen et al. (2004)). In some cases, especially if there is only one change to be detected, the method will "detect" two changes, as required, but it will put one of them near an end of the data sequence, where it can be recognized and ignored. After an initial discovery of one or two change-points, the sequence is broken into two or three parts by those change-points, and the process is iterated as long as new change-points are identified. Here we also consider the statistic $\max_{s<t-h} U_{s,t}$, where

$$U_{s,t} = (V_s, V_t) \Sigma_{s,t}^{-1} (V_s, V_t)'.$$
(18)

and h is a parameter that represents a minimum distance between changes that we find interesting (usually taken to be 5 or 10 in the examples below). An appropriate threshold may be determined from the approximation (closely related to (9))

$$\mathbb{P}\{\max_{s < t} U_{s,t} > b\} \sim \left[2b\varphi(b)/(2\pi)\right] \int_{s < t-h} \det\left[\mathbb{E}(\dot{U}\dot{U}')\right]^{1/2} ds dt. \tag{19}$$

This approximation is approximately linear in the length of the sequence searched, so iterating the process leads in a final step to roughly the same probability of a false positive as is present in the first step. If we assume that in early iterations, only true positives are detected, then the iterative process does not create a multiple comparisons issue. As we will see in the examples below, this method has very good power properties, although its use requires somewhat more thoughtful analysis than the other methods. Since the process Z_t can have relatively large local correlations, when there is only one change to be detected in an interval, and hence we expect to find a second "fake" change near an end-point of the interval searched, that "fake" change may be somewhat distant from the end-point, so it is not clear without additional analysis whether it should be ignored. Use of a linear analysis as in the following section can be very helpful.

A search algorithm based on the maximum of (18) is easily adapted to obtain joint confidence regions for a pair of change points along the lines discussed toward the end of Section 2.1.

An advantage of the top down feature is that the intervals searched are usually relatively long, so it may be reasonable to estimate different values of ρ for the different intervals searched. If we assume that large changes are detected first, this method would presumably reduce the estimated value of ρ , in subsequent searches, but the problem of bias would remain as long as subsequent searches involve intervals containing changes. For the sake of consistency in our examples we have not explored this option.

3.1 Applications.

In this section we consider a number of data sets, where broken line regression is arguably an appropriate model, or at least where it allows one to address questions of interest regarding the times of changes in long term trends. Since all these examples involve observational time series, an assumption of independence seems inappropriate, although in several cases the estimated value of ρ is small enough to be assumed equal to zero.

After employing a detection method, we assume that the detections are in fact correct, so our model becomes a standard linear model. Estimation of the parameters of the linear model gives us an idea of the size and importance of different detected changes, the adequacy of the model as judged by the value of R^2 and $\hat{\rho}$, and the reasonableness of our choice for the value of ρ in our initial segmentation.

Example 3: Greenland temperatures 1901-2016. An example from a site sponsored by the World Bank,

https://climateknowledgeportal.worldbank.org/download-data

is the average annual temperature of Greenland, which may be particularly interesting in view of the large amount of water contained in its glaciers. Data are provided for the years 1901-2016. See Figure 4 in the online Supplement for a plot of Z_t , which suggests a small increase followed by a decrease early in the 20th century, then a second increase near the end of the century. If we use all 116 observations to estimate ρ , we obtain $\hat{\rho} = 0.13$ and the test to detect at least one change detects a decrease in slope occurring in about 1929. If we use only the first half or the second half of the data to estimate ρ , we obtain a value slightly less than 0.1 and with this value detect an increase in 1993. With the smaller estimate of ρ , Seq detects three changes: an increase in 1919, a decrease in 1929, and a second increase that seems to occur about 1973, although 1984 gives essentially the same observed value of

the statistic. With MS, we detect changes in 1929 and 1984. If we set $\rho = 0$, we also barely detect a change in 1919. A linear model incorporating these three changes begins with an initially negative slope, with the first two changes essentially canceling each other, and the third change about three times as large (in magnitude) as the initial negative slope. The effect of putting these changes into the model is to increase R^2 from an initial value of 0.28 to approximately 0.7, while reducing the estimated value of ρ from 0.13 to 0.02, which does not test to be different from 0. Although the change at 1919 is borderline, omitting it from the model provides a less satisfactory result (details omitted).

If we use (18) to search for two changes at a time, we find slope changes in 1918, 1933, and 1983, essentially the same as above.

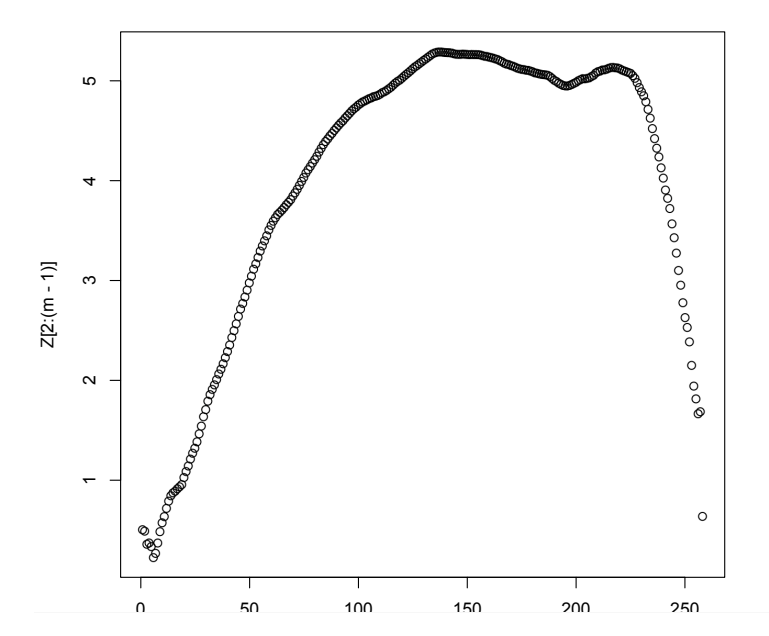
Example 4. Berkeley Earth Central European Temperature Anomalies beginning in 1753. Whereas both the Hadley Center and NOAA provide temperature data, their beginning dates are in the mid to late 19th century, and hence make it difficult to detect slope changes that may have occurred during the 19th century. The Berkeley Earth web site at

provides measurements going back to the mid 18th century. The results for several European countries are quite similar and suggest that at least in Europe increasing temperatures began in the late 19th century before the recent acceleration that began about 1980. As an example we consider Swiss temperature anomalies from 1753 to 2012. Our test for at least one change identifies a slope increase in 1890 with an estimated autocorrelation of 0.24. The plot of Z_t (Figure 2) contains a broad peak and a local maximum in the late 20th century, which suggests the possibility of more than one change. A 95% confidence interval based on the theory suggested above is [1866,1972], which leaves open the possibility of a second change. Seq and MS confirm a 19th century change, but they fail to detect one in

the 20th century even if the autocorrelation is set to 0. With the estimated autocorrelation of 0.24, the statistic (18) detects changes in both 1897 and 1980. A linear analysis with these two change points yields and R^2 of 0.33 and an autocorrelation of 0.03, which does not test to be different from 0. Temperature anomalies of several other countries in Europe exhibit similar, but not identical behavior. In these cases the test to detect a single change will sometimes pick out a local maximum in the 19th century and sometimes in the 20th, while the statistic (18) detects two changes. This is perhaps not surprising since the method was designed for such data. For Switzerland, a 90 % joint confidence region for the two change-points with ρ set equal to 0 contains about 2000 pairs of points. Typical examples near the extremes are (1829,1988), (1888,1962), (1890,1995).

Example 2 (continued): Central England Average Annual Temperature. A challenging case is the central England temperature data for 360 years beginning in 1659. A plot of the data suggests possible changes very early in the series with a much larger change 2-3 hundred years later. The first 80-100 years may be less reliable, due to the primitive thermometers available at that time, but the early data are nonetheless interesting in view of the so-called "little ice age," which overlapped these years. As reported above, a test of at least one change produces a significant increase in slope in 1970 with an estimated autocorrelation of 0.159, and a confidence interval going back about a hundred years, reflecting the increase in the plot of Z_t^2 , in Figure 2, that begins in the late 19th century. If we use Seq with the threshold 4.00 and the autocorrelation 0.159, we find an increase in 1693, a decrease about 1708, and a larger increase about 1890. For MS with a threshold of 4.81 and the same value for ρ , we detect only the change in 1890. If we lower the detection standard to control the global false positive rate at 0.10 and set $\rho = 0.12$, which is the estimate obtained from the first half of the data or from the second half of the data, we obtain a change in 1696 and a

Figure 2: Plot of \mathbb{Z}_t for Berkeley Earth Swiss Temperature Anomalies: 1753-2012.



second in either 1890 or 1988, but without a compelling reason to choose one or the other. Figure 3 suggests that either (or both) could be correct. A linear analysis indicates that the model with only one change at either 1890 or 1988 leads to an R^2 of approximately 0.26 and a value of ρ of about 0.12. Incorporating the two earlier changes detected by Seq raises R^2 to about 0.31 and reduces ρ to about 0.1 for either choice of the third change. Including all four changes raises R^2 to about 0.33 and decreases $\hat{\rho}$ to about 0.08. The statistic (20) to detect two changes at a time detects changes in 1697, 1704, 1730, and 1886; but a linear analysis indicates that the change in 1730 need not be included. The two earlier changes are detected on the initial search, and hence this represents an example where the statistic (20), when faced with an interval where there is only one change, may place a second change sufficiently far from an end-point of the interval searched that it is not obvious that it should be disregarded.

Example 5: Age specific suicide rates in the United States. A small sample size example is suicide rates in the US from 1990 through 2017, which can be found on the web site

ourworldindata.org.

Autocorrelation appears to be very small, so we assume it is 0. All methods detect a substantial slope increase about 2000. For MS this is the only change detected, and it produces an R^2 of 0.91. Seq detects in addition, a second increase about 2014. The statistic (18) detects three changes, a decrease in slope about 1995 before a larger increase in 1999, and a third increase in 2014. A linear analysis with all three changes yields an R^2 of 0.97.

4 Detection of Jump Changes

We consider again the model (2), now with μ_u an unknown constant and $f(u) = \mathbf{1}\{u > 0\}$, so the t_k are change-points in the level of the observed process. For some applications it may seem more appropriate to use $f(u) = \mathbf{1}\{0 < u/\tau \le 1\}$, so the length of a local interval where the mean changes is an unknown constant τ , which may vary from one interval to another when there are multiple changepoints. Since the case $\rho = 0$ has been widely studied, here we concentrate on time series, where the first order autoregressive dependence discussed above may be pertinent. Again it turns out that change-points introduce bias into the estimation of ρ , so we consider estimators based on subsets of the data that appear to be free of change-points.

We consider primarily methods taken from Fang, Li and Siegmund (2018), which, as noted above, motivate the structure of the bottom up segmentation methods suggested in this paper.

We also consider the top down method of circular binary segmentation (CBS) (Olshen et al. (2004)), which may have advantages when a change that increases (decreases) the mean value tends to be followed by a change that decreases (increases) the mean, since it directly models such paired change-points. And finally we consider the analogue of (18), which was not studied in Fang, Li and Siegmund (2018). To that end we take $\rho = 0$ for simplicity and let $S_t = \sum_{1}^{t} Y_u$. Then $V_t = (tS_m/m - S_t)$, so $U_{s,t}$ is defined by the equation (18) for the approximately modified covariance matrix with entries s(1 - t/m) for $s \leq t$. In this section we continue to refer to this as the statistic (18).

Two interesting climate related time series are AMO (Atlantic Multidecadal Oscillation), for which there are data beginning in 1856, and PDO (Pacific Decadal Oscillation) with data from 1900. In both cases the data have been recorded monthly, but we average

the monthly data to get annual time series with 163 and 118 values, respectively.

A visual inspection of the AMO data suggests that there is no change-point before about 1900, so we estimate ρ from the first 45 observations to get the value 0.38. All methods agree that there is a decrease in the mean at 46 (1901), an increase at 70 (1925), a decrease about at 108 (1963), and the latest increase at 139 (1995). A linear analysis with these change-points returns an R^2 of about 0.72 and an auto-correlation of 0. It may be interesting to observe that the changes in slope detected in the Northern Hemisphere ocean temperature anomalies (Example 6 in Section 3.1) fall very close to the mid-points of these three intervals.

The PDO data are similar, but changes appear to be more frequent, as the name suggests, and a cumulative sum plot appears very noisy. If we estimate ρ by all the observations, we get 0.55 and detect no changes. If we use the observations from 1 to 45, we get $\hat{\rho} = 0.30$ and detect changes at 48, 76, 99, and 114 by the pseudo-sequential method and by CBS, while the stricter segmentation method that uses all possible background intervals detects changes at 48, 76, and 114. The statistic (18) detects only the first two change-points. A linear analysis with the four detected change-points produces an R^2 of 0.48 and an estimate for ρ of 0.27.

For these data level changes seem to alternate positive and negative directions, so CBS and related methods that look for paired changes appear to have an advantage. Although the pseudo-sequential method detected the same changes in the PDO data as CBS, its detections at 76 and 114 were borderline.

5 Non-Gaussian Models.

It is relatively straightforward to extend the analysis given above to generalized linear models, at least for independent observations. For example, suppose that Y_u has the log likelihood

$$Y_u \theta_u - \psi(\theta_u), \tag{20}$$

where

$$\theta_u = \mu_u + \xi f(u - t).$$

The efficient score to test the hypothesis $\xi = 0$ or segment the sequence is much as before, although computation of $\Psi(t)$ is more complicated. Fortunately at least for the following examples, it seems plausible to assume independent (quasi)Poisson observations.

A perhaps more flexible model than (20) is an asymptotic quasi-likelihood model, e.g., Heyde (1997), where there is the possibility of different models for the mean and variance. A very similar model to the one we developed in Section 2 is obtained by setting $\psi(\theta_u) = \theta_u^2/2$ in (20), but we interpret θ_u as the conditional expectation of Y_u given the observations up to u-1, so the efficient score to detect a local signal is a sum of martingale differences. It is then straightforward to extend the methods developed above.

Example 6: Rain Storms in New Zealand An example modeled as jump changes in a Poisson mean are heavy rain storms in New Zealand since 1900, which have been catalogued at https://hwe.niwa.co.nz.

Both Seq and (18) suggest that there are two periods of increased storm activity—from about 1920 to approximately 1949 and from 1996 to 2010. The statistic MS misses the decrease in level in 1949, but detects the other three changes. A generalized linear

model analysis indicates that the four change model is preferable to three changes, but not surprisingly gives a relatively small z-score to the change in 1949.

A series of interesting, but often challenging examples of contemporary interest are the slope changes occurring in the new cases day by day of COVID-19 occurring in various locations. We have used data from

ourworldindata.org

.

Example 7: COVID-19 in Santa Clara County, California. We consider the 72 day history by day ending on 12 April 2020. The statistic (20), initially at a constant mean value and allowing for a slope change and for overdispersion, detects an increase in slope on the 34th day. The quasilikelihood statistic with $\psi(\theta) = \theta^2/2$, autocorrelation of 0 and constant variance for the residuals, i.e., effectively just the single change statistic of Section 2, detects a slope increase on the same day. Both a linear least squares analysis and a log-linear (Poisson) analysis confirm this change and indicate 0 autocorrelation. The dispersion paramter is estimated to be about 20.

Example 8: COVID-19 in South Korea. South Korea provides an example (84 observations as of 12 April, 2020). which involves multiple changes. We use a quasi-likelihood analysis, again with 0 autocorrelation. The statistic Seq detects a slope increase at 27, a decrease at 44, and another increase at 54, all of which seem evident from a plot of the data. The statistic (18) suggests slope changes at observations 32, 41, and 54 while the statistic MS also detects three changes: at 32,44, and 55.

Remark. Additional examples and discussion of COVID-19 data are contained in the online supplement.

6 Discussion.

We have studied several score statistics to detect local signals in the form of changes of level, slope, or (in the online Supplement) the autoregressive coefficient. To segment the observations, we consider two "bottom up" methods patterned after the methods of multiple change-point segmentation in Fang, Li and Siegmund (2018) and one "top down" method, defined in (18).

Estimation of the nuisance parameters, ρ and σ^2 , pose special problems. For the bottom up methods, in examining an interval of observations for possible change-points, intercept, level, slope and variance of the process are estimated locally, i.e., using only the data from the interval under consideration. For the autoregressive coefficient, our theory suggests using the (global) maximum likelihood estimator estimator under the hypothesis of no change. Since this estimator can be badly biased and result in a loss of power when there are change-points, we also consider ad hoc methods based on examination of different parts of the data. For use of (18), which estimates of σ^2 based on the (usually long) interval being searched, a possible method for dealing with variance heterogeneity arising from the early part of the data is to discard initial segments of varying length and consider the stability of the results obtained.

The multiple regression analsis suggested in Section 3.1, based on the assumption that detected break-points are correct, allows us to see if our segmentation is reasonable, estimate the magnitude of the detected signals, and reconsider our chosen value of ρ to see if we have used one that is too small. In most examples, it appears that we have used a larger value than necessary, which may result in a loss of power in the case of a large discrepancy.

A different approach would be to use initially the value $\rho = 0$, or some other small value to detect change points, apply the multiple regression analysis to discard changes

that seem to be superfluous, and then iterate the process with the value of ρ suggested by the regression analysis. We have not chosen this path because our goal has been to use a value of ρ obtained with at most a small amount of "data snooping," in order to claim that due to minimal re-use of the data the false positive error rate has been adequately controlled.

Because our emphasis has been on detection of local signals, we have admittedly been selective in our use of examples and for the most part have limited our subsequent linear analysis to what it can tell us about our detection methods. In some examples it seems interesting to ask if there are explanations for the local changes: e.g., what is the evidence that a temperatures began to increase in the late 19th century, perhaps accompanied by an hiatus in the early-mid 20th century, before accelerating about 1980? In other examples it appears that our methods may lead to a reasonable regression fit without suggesting that the detected change-points need an explanation.

For problems involving sparse, bump like changes as discussed briefly the Supplement, some superficial analysis suggests that our methods work well since most of the data are consistent with the null model, and hence global estimation of nuisance parameters does not pose a serious problem. In view of the ubiquity of genomic applications where "bumps" have different signatures suggested by a combination of science and experimental technique, and where the background may involve use of a control group it seems worthwhile to pursue a more systematic study.

Here we have considered signals in one-dimensional processes, where the number of possible "shapes" of the signals is relatively small. In view of the much larger variety of possible multi-dimensional signal shapes and the variety of approaches already existing in the literature a systematic comparative study of that problem may be valuable.

References

- R. J. Adler and J. E. Taylor (2007). Random Fields and Geometry Springer-Verlag, New York-Heidelberg-Berlin.
- R. Baranowsk, Yining Chen, and P. Fryzlewicz (2019). Narrowest-over-threshold detection of multiple change-points and change-point-like features *J. Roy. Statist. Soc. B* **89**, 649-672.
- K. S. Chan and H. Tong (1990) On likelihood ratio tests for threshold autoregression JRSSB 52, 469-476.
- R. B Davies (1987). Hypothesis testing when a nuisance parameter is present only under the alternative *Biometrika* **74**, 33-43.
- X. Fang, J. Li and D. O. Siegmund (2018). Segmentation and estimation of change-point models: false positive control and confidence regions *Arkiv*
- P. Fryzlewicz (2014). Wild binary segmentation for multiple change-pont detection. *Ann. Statist.* **42**, 2243–2281.
- C. C. Heyde (1997) Quasi-Likelihood and Its Application Springer-Verlag, New York-Heidelberg-Berlin.
- A. E. Jaffe, A. P. Feinberg, R. A. Irizarry, and J. T. Leek (2012a). Significance analysis and statistical dissection of variably methylated regions. *Biostatistics* 13, 166–178.
- A. E. Jaffe, P. Murakami, Hwajin Lee, J. T. Leek, M. Daniele Fallin, A. P. Feinberg, and R. A. Irizarry (2012b). Bump hunting to identify differentially methylated regions in epigenetic epidemiology studies, *Int. J. of Epidemiology* 41, 200–209.

- P. D. Jones, D. H. Lister, T. J. Osborn, C. Harpham, M. Salmon, and C. P. Morice Hemispheric and large-scale land surface air temperature variations: An extesive revision and an update to 2010. *J. Geophys. Res.* **117** D05127,doi:10.1029/2011JD017139.
- M. Knowles and D. Siegmund (1989) On Hotelling's approach to testing for a nonlinear parameter in regression *Int. Statist. Rev.* **57** 205-220.
- M. Knowles, D. Siegmund and H. P. Zhang (1991) Confidence regions in semilinear regression *Biometrika* **79** 15-31.
- C. Loader (1992). A log-linear model for a Poisson process change-point. *Ann. Statist.* **20** 1391-1411.
- Gordon Manley (1974) Central England temperatures:monthly means 1659 to 1973 Quarterly J. Roy. Meteorological Soc. 100 389-405.
- V. M. R Muggeo (2016) Testing with a nuisance parameter present only under the alternative: a score based approach with application to segmented modeling *J. Statistical Computation and Simulation* doi: 10.1080/00949655.2016.1149855
- A. B. Olshen, E. S. Venkatraman, R. Lucito and M. Wigler (2004). Circular binary segmentation for the analysis of array-based DNA copy number data. *Biostatistics* 5, 557–572.
- A. E. Raftery and V. E. Akman (1986). Bayesian analysis of a Poisson process with a change-point. *Biometrika* **73**, 85–80.
- M. W. Robbins, C. M. Gallagher, and R. Lund (2016). A general regression change-point test for time series data, *Jour. Amer. Statist. Assoc.* **111** 670–683.

- A. Schwartzman, A. Jaffe, Y. Gavrilov, Y. and C. E. Meyer (2013). Multiple testing of local maxima for detection of peaks in ChIP-seq data, *Ann. Appl. Statist.*, 7, 471-494.
- H. Shin, T. Liu, X. Duan, Y. Zhang, X. S. Liu (2013). Computational methodology for ChIP-seq analysis. *Quantitative Biology* 1, 54–70.
- D. O. Siegmund and K. J. Worsley (1995). Testing for a signal with unknown location and scale in a stationary Gaussian random field. *Ann. Statist.* **23**, 608–639.
- A. F. M. Smith and D. G. Cook (1980). Strait lines with a change-point: an analysis of some renal transplant data *J. Roy. Statist. Soc. Series C* **29**, 180-189.
- J. D. Toms and M. L. Lesperance Piecewise regression: a tool for identifying ecological thresholds *Ecology* **84**, 2034-2041.
- N. R. Zhang, D. O. Siegmund, H. Ji and J. Z. Li (2010). Detecting simultaneous change-points in multiple sequences. With supplementary data available online. *Biometrika* 97, 631–645.

SUPPLEMENTARY MATERIAL

Appendix A: Some Basic Calculations

In this appendix we record basic formulas we have used in the paper. Assume the model is given by (2) with M=1 and $\mu_u=\alpha+\beta[(u-(T+1)/2)/T]$. The expressions given below are asymptotic for T>>1; and for some specific examples, the results used are computed in continuous time. Hence, for example, $\sum_{u=1}^{T} f[(u-t)/T]$ may be evaluated as $T \int_0^1 f(u-t/T) du$, and $\mathbb{E}(Y_u)$ may be computed after solving the differential equation (3). In the change-point problems of (Fang, Li and Siegmund (2018)), where the function f is discontinuous, use of a continuous time model would result in considerable loss of accuracy, but it seems much less consequential here where for many of our examples, in particular for broken line regression, the stochastic processes under consideration have piecewise differentiable sample paths. Let $\gamma = 1 - \rho$. Then

$$Y_u = (\sum_{j>0} \rho^j)[\alpha + \beta(u/T - 1/2]) + \sum_{j>0} \rho^j \epsilon_{u-j} + O_p(1/T),$$
(21)

or alternatively the solution of (3) with $Y_0 = 0$ is

$$Y_u = \int_0^u \exp[-\gamma(u-s)]\{(\alpha + \beta(s/T - 1/2) + \xi f[(s-t)/T])ds + dW(s)\}.$$
 (22)

Hence, under the null hypothesis that $\xi = 0$ we have

$$\Psi(t)' = \mathbb{E}(\ell_{\xi}\ell_{\theta})' \sim T(1, 1/12, (1-\rho)^{-1}[\alpha + \beta/12].$$

Let $\Delta_u = Y_u - \rho Y_{u-1} - \alpha - \beta(u - T/2)$. The ingredients of the representation $Z_t = [\ell_{\xi}(t) - \Psi(t)'A\ell_{\theta}]/\sigma(t)$ introduced in Section 2 are

$$\ell_{\xi}(t) = \sum_{u} \Delta_{u} f[(u-t)/T];$$

$$\ell_{\theta} = (\sum_{u} \Delta_{u}, \sum_{u} \Delta_{u}[(u - (T+1)/2)/T], \sum_{u} \Delta_{u}Y_{u-1})';$$

$$\Psi(t) \sim (\sum_{u} f[(u-t)/T], \sum_{u} f[(u-t)](u/T - 1/2), \sum_{u} \{f[(u-t)/T](\alpha + \beta[(u-T)/(2T)]\}/(1-\rho))'.$$

For the special case of broken line regression in continuous time the first and second coordinates are respectively $g_1(t,T) = (T-t)^2/2T^2$, $g_2(t,T) = [(T-t)^3/12 - t(T-t)^2/4]/T^3$.

The matrix $A^{-1} = \mathbb{E}(\ell_{\theta}\ell'_{\theta})$ is straightforward to compute and somewhat tedious to invert. A very useful result is

$$\Psi(t)'A = \left(\sum_{u} f[(u-t)/T], \sum_{u} f[(u-t)/T][(u-1/2)/T] / \sum_{u} (u/T - 1/2)^{2}, 0\right). \tag{23}$$

It follows that the numerator of Z_t , has covariance function

$$\Sigma(s,t) \sim \sum_{u} f[(u-s)/T]f[(u-t)/T] - \Psi(s)'A\Psi(t),$$
 (24)

which does not depend on α , β , nor on ρ . In particular

$$\sigma^{2}(t) \sim \sum_{u} f[(u-t)/T]^{2} - \Psi(t)'A\Psi(t).$$
 (25)

To derive (15) and (17) (see below), we must consider T as variable and study the quantities σ^2 , Ψ , etc., as functions of both t and T. It is obvious from (25) that $\partial \sigma^2(t,T)/\partial T$ does not depend on nuisance parameters. Since $\Psi(t,T)$ depends on the nuisance parameters (α, β, ρ) only in its third coordinate, if we first differentiate (23) with respect to T, then multiply on the right by $\Psi(t,T)$ it follows from (23) that neither $(\partial \Psi/\partial T)'A_T\Psi(t,T)$ nor $\Psi(t,T)'(\partial A_T/\partial T)\Psi(t,T)$ depends on nuisance parameters. The approximation (17) requires that we introduce $T_0 < t$ as a third parameter. For broken line regression we also require

$$\Psi' A \partial \Psi / \partial T_0 = -3T^3 (1 - t/T)^2 g_2[(t - T_0)/T, (T_1 - T_0)/T]/(T_1 - T_0)^3.$$
 (26)

To study the behavior of Z_t when ξ is different from 0, and to help with the interpretation of a plot of Z_t , we put $t = (t_1, \ldots, t_k)$, $\xi = (\xi_1, \ldots, \xi_k)$ and use the notation $\mathbb{E}_{t,\xi}(\cdot)$. By combining the results given above we find that

$$\mathbb{E}_{t,\xi}(Z_s) = \sum_{j} \xi_j \Sigma(t_j, s) / \sigma(s). \tag{27}$$

Appendix B: Additional Broken Line Examples.

Example 9: Reconstruction of Global Sea Levels. We consider the reconstruction of Church and White (2011) of global sea levels beginning in 1880. An updated version of the data can be found at

https://github.com/datasets/sea-level-rise/blob/master/archive/

Our test for at least one change detects a slope increase in 1991. See Figure 5, where the broad peak of the plot of Z_t suggests there may be more than one change-point. The estimated autocorrelation based on all the data is 0.34, and with this estimate Seq detects slope increases in 1938 and 1999. With the same estimate of ρ MS detects only the change in 1999. However, in the first 100 observations the estimated autocorrelation is only 0.14. With an autocorrelation of 0.25 for MS, slope changes are detected in 1935 and 2000. A linear model incorporating these two changes yields an R^2 greater than 0.99 and an estimate for ρ of 0.06. With $\rho = 0.34$ the test (18) to detect two changes at a time indicates in addition to slope increases in 1932 and 1991 a decrease in 1915. With these three changes a linear analysis gives approximately the same R^2 and ρ as the model with only two changes.

Example 10: Northern Hemisphere Ocean Temperature Anomalies. An interesting example is provided by time series of ocean temperature. Both NOAA and the Hadley Center provide relevant data. The northern hemisphere temperatures appear to be an interesting illustration of our methods since a plot of the data suggests the possibility of multiple changes during the 20th century. We first consider the NOAA monthly anomalies, with m = 1665.

ftp://ftp.ncdc.noaa.gov/pub/data/noaaglobaltemp/operational/timeseries/

Our test for at most one change gives a p-value about 0.001 and an estimated autocorrelation of 0.94 (cf. Figure 6). Since estimates of ρ based on segments of the data that appear not to involve changes were no more than 0.9, we tried using Seq with that value of ρ and a threshold equal to the nominal 0.05 threshold of 4.40. At these settings an increase was detected at observation 367 months (1912), a decrease at 756 (1943), and a second increase at 1133 (1974). For the m=139 average annual anomalies, where ρ appears to be substantially smaller, at a threshold of b=3.75, $m_0=4$, and ρ set equal to 0.5, positive changes are detected in 1910 and 1975, with an intervening negative trend in 1943. At the conventional level 0.05, MS detects the first and the third of these change-points, but misses the second. For the annual average northern hemisphere ocean temperature anomalies a linear model without changes has an R^2 of 0.88. Incorporating the three slope changes detected by Seq into the model produces only a small increase in R^2 to 0.90, but a large decrease in the estimated value of ρ from 0.80 to 0.52. The statistic (18) also suggests three changes in slope, at 1909,1941, and 1974. For these changes the linear model again gives and R^2 of 0.90 and estimates ρ to be 0.47.

Example 11: Atmospheric Greenhouse Gases. In view of their connection with global warming, it is interesting to consider atmospheric greenhouse gases. Systematic atmo-

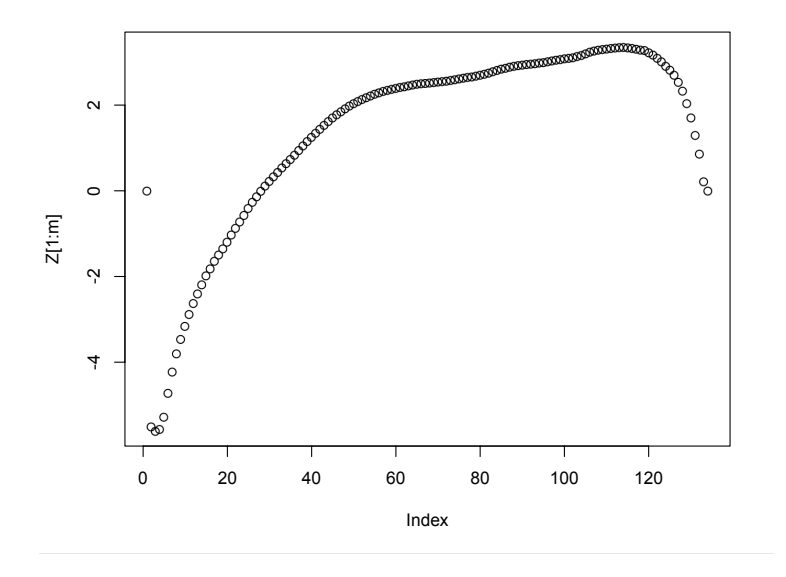


Figure 3: Plot of Z_t for reconstructed sea level rise from 1880 to 2014.

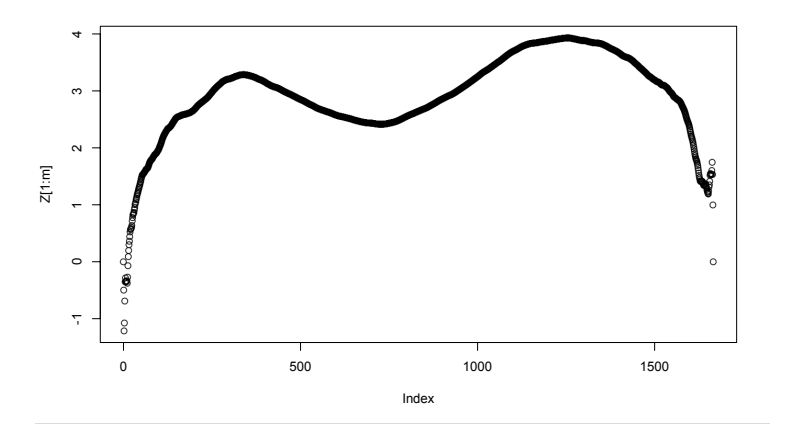


Figure 4: Plot Z_t , NOAA northern hemisphere ocean anomalies.

spheric measurements began relatively recently, although reconstructions from surrogate measurements go back centuries. Atmospheric measurements for CO₂ show a number of increases in slope since about 1960. To illustrate our methods, we first consider global average methane emissions for 35 years beginning in 1984, reported at

A linear model without changes shows a positive slope with an R^2 of 0.95 and an autocorrelation of zero. MS detects a slowing of the rate of increase in 1993 followed by a large increase in 2010. Incorporating these changes into a linear model produces an R^2 greater than 0.99 and an autocorrelation of zero. The statistic (18) detects the same two changes, although it places the initial decrease about 1996.

An example of surrogate measurements of atmospheric CO_2 is provided by the web site of the Institute for Atmospheric and Climate Science (IAC) at the ETH-Zürich.

To provide a comparable time frame to Example 3, we consider the 260 years 1755-2014. Unlike other examples, where changes are difficult to detect because of large variability, the variability in these data (and in the recent atmospheric measurements) is very small, so there appear to be many small changes, that do not help us to understand larger patterns that may have environment impact. The top down statistic (18) focuses on relatively few, large changes. The null estimate of ρ is 0.39. With this value the first two changes suggested by (18) are slope increases occurring in 1871 and 1959. A linear model with these change-points produces an R^2 of 0.995 and a estimated value of ρ of 0.01. The statistic MS with the same value of ρ and $T_0 = 20$ to deter detection of small changes, detects the large increase in 1959 and an earlier detection in 1853, which has roughly the same effect on the linear model as the change in 1871 detected by (18). Both statistics suggest that there

are additional small changes in the first hundred years. The statistic (18), but not MS, suggests there may be a slope decrease in 1943, which together with the two other changes detected increases R^2 to 0.997. This change may be interesting insofar as it appears to coincide roughly with the hiatus in temperature increases in Greenland shown in Example 3 and the dip in northern hemisphere ocean anomalies mentioned in Example 10.

Appendix C: Bump Hunting: fixed shape, variable amplitude and scale.

In a variety of problems, the local signal to be detected occurs in a departure from, followed by a return to, a baseline value. In many cases the shape of the local signal arises naturally from the scientific context. An important example is inherited copy number variation, where there is an abrupt increase or decrease from the baseline value of two, which is followed quickly by a return to the baseline (e.g., Zhang et al. (2010)). Other examples are ChIP-Seq, where a shape to expect is roughly triangular or double exponential (e.g., Shin et al. (2013)), or differential methylation, where a normal probability density function or an integral thereof might be reasonable (cf. Jaffe, et al. (2012a)).

We modify (2) to include a scale paramter τ , to obtain the log likelihood function

$$-.5\sum_{1}^{T} [Y_u - \rho Y_{u-1} - \mu_u - \sum_{k} \xi_k f\{(u - t_k) / \tau_k\}]^2.$$
 (28)

Here f is a positive, symmetric integrable function, e.g., the square root of (i) a standard normal density function, (ii) a triangular probability density on [-1,1], (iii) a double exponential probability density, or (iv) a uniform probability density function on [-1/2, 1/2]. Consider the case of at most one bump and assume that the search interval is long enough relative to the scale parameter that it is reasonable to ignore end effects. We define our standardized statistic as above, but we now write it as $Z_{t,\tau}$ to reflect the unknown location t and width τ of the bump. An approximation to its false positive error probability is

given in display (9). (For (iv) above a different approximation is required because of the discontinuities in f. See Fang, Li and Siegmund (2018).)

Often bumps are relatively sparse, which makes estimation of ρ and σ^2 relatively easy, so one can see intervals of the data that can be used for estimating autocorrelation and other nuisance parameters without serious bias.

Although a serious study of these methods is warranted by the variety of potential applications, we do not discuss these in detail here, which would require a lengthy investigation of the specific scientific features of those applications.

Appendix D: Additional COVID-19 Examples.

Example 11. COVID-19 in Italy. An interesting example is Italy, which had substantial difficulty in controlling the spread of the virus. Using data for 74 days up to (including) 12 April 2020, we find that MS detects changes an increase at day 34 and a substantial decrease at day 53. A linear least squares analysis and a (quasi) Poisson analysis suggest that these changes are reasonable.

Example 12. COVID-19 in Hong Kong An extremely well organized and informative web site is

chp-dashboard.geodata.gov.hk/covid-19/en.html

.

For 80 days of data up to 12 April, 2020, the method MS detects an increase in new cases on the 52nd day, followed by a decrease on the 66th. Both a least squares linear analysis and a (quasi)Poisson analysis suggest these are reasonable, with no day to day autocorrelation. Results for Taiwan are similar.

Example 13. COVID-19 in China In addition to South Korea, discussed above, China is another country that has apparently managed to stop the epidemic, but it poses a special

challenge because the data are very noisy and contain one huge outlier in the center of the sequence of observations. To mitigate the effect of this outlier, we assumed that there had been a reporting delay and arbitrarily distributed many of those cases between the preceding two days. For the 97 days before 6 April 2020, Seq detects three changes at days 20, 46, and 55, while (18) would place them at 24, 45, and 54. Both the least squares linear analysis and a generalized linear (quasi)Poisson analysis seem to approve of these results. MS also detects three changes, at slightly different locations. Results for Taiwan are quite similar.

The COVID-19 data typically start with a small number of cases showing relatively little day to day variability. When the number of cases is larger, the variability also becomes larger. In some cases it is enormous, apparently partly due to reporting delays that can lead to huge fluctuations in a one or two days interval. The bottom up methods, Seq. and MS seem to control the false positive rate reasonably well, because they estimate the variance of the data locally. In contrast (18) estimates the variance globally—according to the interval searched, so it may make false positive errors by using a variance that is too small. However, its stability can be checked by looking for consistency when the starting point of the sequence is varied. There are limitations, since starting the search too late in the sequence makes it difficult to detect an early change. To avoid some of the reporting incongruities, it is tempting to use a moving average of the day to day data. This reduces the variance but increases the autocorrelation quite substantially. In a small number of numerical experiments, it did not seem to offer consistent advantages. An interesting feature of our linear least squares analysis of the detected changes is that the estimated slopes are additive, so we have some information about the danger of another flare-up. In both the South Korean and the China data, the net slope change is close to zero. It

may be interesting to consider a (quasi)Poisson log linear analysis, which usually agrees with the linear least squares analysis. The dispersion parameter often indicates large over-dispersion. We have also considered a detection strategy using a square root transformation of the dependent variable, which would be expected to stabilize Poisson like variability. Simulations suggest that this technique can be useful, but also that heteroscedasticity is usually not a serious problem.

Appendix E: Threshold Autoregression

As a final illustration of our methods we consider a simple case of Threshold Autoregression, which has been studied in a number of papers by Tong and colleagues.

For a model assume

$$Y_u = \mu + \rho Y_{u-1} + \xi Y_{u-1} I\{Y_{u-1} \le t\} + \epsilon_u \tag{29}$$

To test $\xi = 0$, in the notation of Section 2

$$\ell_{\xi}(t) = \sum_{u} (Y_u - \mu - \rho Y_{u-1}) Y_{u-1} I\{Y_{u-1} \le t\},$$

and asymptotically under the null hypothesis we have

$$\Psi(t)' \sim T(\mathbb{E}(Y; Y \leq t), \mathbb{E}(Y^2; Y \leq t)),$$

$$\dot{\ell}_{\theta} = (\sum (Y_u - \mu - \rho Y_{u-1}), \sum (Y_u - \mu - \rho Y_{u-1}) Y_{u-1}),$$

and A^{-1} is the 2 × 2 matrix with entries $a_{11} = T$, $a_{12} = T\mathbb{E}(Y)$, $a_{22} = T\mathbb{E}(Y^2)$, where Y denotes the stationary distribution of Y_u under the null hypothesis (and the stationarity assumption that $|\rho| < 1$). Hence

$$\sigma^2(t) \sim T\mathbb{E}(Y^2; Y \le t)$$

$$-T[\mathbb{E}^{2}(Y^{2}; Y \leq t) + \mathbb{E}(Y^{2})\mathbb{E}^{2}(Y; Y \leq t) - 2\mathbb{E}(Y)\mathbb{E}(Y; Y \leq t)\mathbb{E}(Y^{2}; Y \leq t)]/\mathbb{V}ar(Y). \quad (30)$$

Let $G(t) = \mathbb{E}(Y^2; Y \leq t)$, so $\sigma^2(t) \sim T[G(t) - \Psi(t)'A\Psi(t)]$. Straightforward calculations show that the covariance of the standardized score statistics Z_s and Z_t are given by $[G(\min(s,t)) - \Psi'(s)A\Psi(t)]/\sigma(s)\sigma(t)$. Hence locally for small δ

$$\mathbb{C}ov(Z_t, Z_{t+\delta}) \approx I - (\delta/2)[G - \Psi'A\Psi]^{-1}\dot{G},$$

where the functions G, Ψ and \dot{G} are evaluated at t, and slightly more generally $\mathbb{C}ov[(Z_{t+\delta_1}, Z_{t+\delta_2})|Z_t] \approx \min(\delta_1, \delta_2)[G - \Psi'A\Psi]^{-1}\dot{G}$. This allows us to calculate an approximation to $\mathbb{P}\{\max_t |Z_t| \geq b\}$. The methods of, e.g., Woodroofe (1976) or Yakir (2013) lead after some calculation to

$$\mathbb{P}\{\max_{t_0 < t < t_1} |Z_t| > b\} \approx 2b\varphi(b) \int_{t_0}^{t_1} [\Psi'(t)A\dot{\Psi}(t)/\sigma^2(t)]dt. \tag{31}$$

We have evaluated (31) by numerical integration, and the p-values given below come from that evaluation with the observed mean value and standard deviation. We have also implemented an empirical version of this approximation, where the entire computation is based on the appropriately estimated quantities. These two approximations are in rough agreement for our examples, where the p-value is very small. Simulations suggest that the Type I error control of (31) is adequate under the model The power also seems reasonable. In principle, one should learn something from the maximizing point of the statistic Z_s relative to the estimated values of μ and of σ , but in simulations the maximizing value of shows more variability than we can easily interpret. A calculation similar to that giving (30) indicates that in the case that $\xi \neq 0$ the expected value of Z_t is approximately $\xi T^{1/2}\sigma(t)$, as it would be for likelihood theory with standard regularity conditions. This approximation seems relatively stable and suggests a rough approximation for ξ by equating the approximation to the observed value of $\max_s Z_s$ (or $\min_s Z_s$).

With a slight modification in principle, but substantially more detailed calculation in application, one can consider higher order autoregressions. Suppose, for example, the model is

$$Y_u = \rho_1 Y_{u-1} + \rho_2 Y_{u-2} + (\xi_1 Y_{u-1} + \xi_2 Y_{u-2}) I\{Y_{u-2} \le t\} + \epsilon_u.$$

Now X_t is a two-dimensional vector, while G(t), $\Psi(t)$, and $\sigma^2(t) = \Sigma_t$, say, are 2×2 matrices. An appropriate test statistic has the form $\max_t V_t' \Sigma_t^{-1} V_t$. Putting $Z_t = \Sigma^{-1/2} V_t$, we can control the false positive probability based on the approximation

$$\mathbb{P}\{\max_{t_0 < t < t_1} ||Z_t|| > b\}$$

$$\approx (b^2/2) \exp(-b^2/2)(2\pi)^{-1} \int_{t_0}^{t_1} \int_0^{2\pi} \mathbf{e}' \Sigma_t^{-1} \dot{G}(t) \mathbf{e} d\omega dt + \exp(-b^2/2), \tag{32}$$

where $\mathbf{e} = (\cos(\omega), \sin(\omega))'$, and where π^{-1} times the integral over ω equals the trace of $\Sigma_t^{-1} \dot{G}(t)$.

Simulations suggest that the Type I error control of this procedure is adequate under the model. The power also seems reasonable. In principle, one should learn something from the maximizing point of the statistic Z_t relative to the estimated values of μ and of σ , but in simulations the maximizing value of t shows more variability than we can easily interpret.

Examples. As illustrative applications, we follow Chan and Tong (1990) in considering the Canadian lynx data and Nicholson's blowfly data. We do not, however, try to give a complete discussion of these well studied data.

The Canadian lynx data consist of annual counts over a 114 year period, which are considered a surrogate for the size of the lynx population. The scientific reasoning behind a two-phase model is the hypothesis that when the lynx population is small, it finds a more

than adequate food supply and increases until it reaches a size where the food supply is inadequate, when it then decreases until the cycle begins again. Empirical observations suggest that the decrease in times of food shortage is more rapid than the increase in times of abundance. If we use a first order auto regressive model, these fluctuations suggest a positive autoregressive parameter in times of food abundance, which decreases when there is a food shortage. Although there are clear outliers in the data, which has lead others to consider transformations to shorten the tails, we analyze the original data. Employing the first order autoregressive model with a possible change in the autoregressive parameter, as suggested above yields null estimators of $\mathbb{E}(Y)$ and $\mathbb{V}ar(Y)$ of 1538 and 1560, respectively. The maximum value of Z_t is 3.89, which occurs at about t = 3500, and the resulting (two-sided) p-value based on (31) is approximately 0.004.

Nicholson's blowfly data (Brillinger (et al. 1980) and the web site

www.stat.berkeley.edu/brill/blowfly97I.html

contains 361 observations in four columns, labeled respectively "births," "nonemerging," "emerging," and "deaths." The first, third, and fourth columns vary from numbers close to 0 to numbers in the several thousands. The second column typically involves substantially smaller numbers. For the first column. the estimated mean value, autocorrelation, and standard deviation under the null model are 1438, 0.6 and 1670, respectively. The maximum Z value is about 4.73, which occurs for $t \approx 5300$. The p-value for the hypothesis of no change is approximately 2×10^{-4} . For "emerging" the maximum Z-value is about 5.22, which gives a p-value of about 6×10^{-5} . For these data the change in the autocorrelation is positive.

References

- D. R. Brillinger, J. Guckenheimer, P. Guttorp and G. Oster (1980) Empirical modelling of population time series data: the case of age and density dependent vital rates *Lectures* on Mathematics in the Life Sciences 13, 65-90 American Math. Soc.
- K. S. Chan (1991) Percentage points of the likelihood ratio test for threshold autoregression JRSSB 53, 691-696.
- K. S. Chan and H. Tong (1990) On likelihood ratio tests for threshold autoregression JRSSB 52, 469-476.
- J. A. Church and N. J. White (2011) Sea level rise from the late 19th to the early 21st century Surv. Geophysis. 32, 585-602.
- A. E. Jaffe, A. P. Feinberg, R. A. Irizarry, and J. T. Leek (2012a). Significance analysis and statistical dissection of variably methylated regions. *Biostatistics* 13, 166–178.
- A. E. Jaffe, P. Murakami, Hwajin Lee, J. T. Leek, M. Daniele Fallin, A. P. Feinberg, and R. A. Irizarry (2012b). Bump hunting to identify differentially methylated regions in epigenetic epidemiology studies, *Int. J. of Epidemiology* 41, 200–209.